

LHC and B physics probes of neutrinoless double beta decay in supersymmetry without R-parity

B. C. Allanach¹, C. H. Kom^{1,2}, H. Päs³

¹ DAMTP, University of Cambridge, Wilberforce Road, Cambridge, CB3 0WA, UK

² Cavendish Laboratory, J.J. Thomson Avenue, Cambridge CB3 0HE, UK

³ Fakultät für Physik, Technische Universität Dortmund, D-44221, Dortmund, Germany

E-mails: b.c.allanach@damp.cam.ac.uk, kom@hep.phy.cam.ac.uk,
heinrich.paes@uni-dortmund.de

ABSTRACT: In the minimal supersymmetric extension to the Standard Model with R-parity violation, a non-zero coupling λ'_{111} predicts both neutrinoless double beta decay and single selectron production at the LHC. We show that, in this case, if neutrinoless double beta decay is discovered in the next generation of experiments, there exist good prospects to observe single selectron production at the LHC. The coupling product $\lambda'_{113}\lambda'_{131}$ can contribute towards neutrinoless double beta decay through both heavy sbottom exchange and standard light Majorana neutrino exchange. We study how complementary processes from heavy flavour physics and resonant single selectron production at the LHC can shed light on which decay mechanism is dominant.

KEYWORDS: Supersymmetry Phenomenology, Neutrino Physics, B-Physics, Collider Physics.

Contents

1. Introduction	1
2. Mechanisms of $0\nu\beta\beta$ in the RPV MSSM	4
2.1 Light Majorana neutrino exchange: $0\nu\beta\beta$ via $m_{\beta\beta}$	4
2.2 Heavy sbottom exchange: $0\nu\beta\beta$ via $\lambda'_{113}\lambda'_{131}$	5
2.3 Heavy sparticle exchange: $0\nu\beta\beta$ via $\lambda'_{111}\lambda'_{111}$	6
3. Experimental limits and nuclear matrix elements	8
4. Implications of $\lambda'_{113}\lambda'_{131}$ bound from $B_d^0-\bar{B}_d^0$ on $0\nu\beta\beta$ in mSUGRA	13
5. Single selectron production at the LHC via λ'_{111}	16
6. Discussion and summary	19
A. Neutralino decays with RPV couplings associated with the neutrino mass scale	21

1. Introduction

Neutrinoless double beta decay ($0\nu\beta\beta$) provides the most sensitive probe to both lepton number violation as well as a Majorana nature of neutrinos. At the quark level, this process corresponds to the simultaneous transition of two down quarks into two up-quarks and two electrons. While the most prominent mechanism triggering this decay involves the exchange of a massive Majorana neutrino, several other possibilities have been discussed in the literature, including an attractive alternative being mediated by the exchange of sparticles in supersymmetric models with R-parity violation [1–5].

In supersymmetric extensions to the Standard Model (SM), the most general superpotential contains baryon- and lepton- number violating operators at the renormalisable level. The presence of both sets of operators typically leads to violation of stringent bounds on proton decay [6], unless the parameters are unnaturally suppressed. This problem can be avoided if a discrete symmetry is imposed which forbids at least one set of such parameters. A widely-studied example is so-called R-parity [7], under which both sets of operators are odd under the parity transformation and hence are forbidden. This symmetry also has the advantage of having the lightest supersymmetric particle (LSP) as a natural dark matter (DM) candidate. On the other hand, there exist R-parity conserving (RPC) dimension 5 operators which could potentially lead to fast proton decay [8, 9].

Instead of R-parity, we focus on an alternative, namely baryon triality¹ [10, 11]. This \mathbf{Z}_3 discrete symmetry allows for the dimension 4 R-parity violating (RPV) terms which violate lepton number, while those that violate baryon number are forbidden. A significant advantage of this class of models is that proton decay is forbidden also at dimension 5. On

¹Also known as baryon parity in some literature.

the other hand the LSP will decay via the non-zero RPV couplings present. In the rest of this paper, we use the term R-parity violation to denote the lepton number violating, R-parity violating interactions.

The chiral superfields of the minimal supersymmetric extension to the Standard Model (MSSM) are charged under the SM gauge group $G_{SM} = SU(3)_c \otimes SU(2)_L \otimes U(1)_Y$ as

$$\begin{aligned} Q &: (3, 2, \frac{1}{6}), & \bar{U} &: (\bar{3}, 1, -\frac{2}{3}), & \bar{D} &: (\bar{3}, 1, \frac{1}{3}), \\ L &: (1, 2, -\frac{1}{2}), & H_d &: (1, 2, -\frac{1}{2}), \\ \bar{E} &: (1, 1, 1), & H_u &: (1, 2, \frac{1}{2}), \end{aligned} \quad (1.1)$$

where all family indices are suppressed. The renormalisable RPV MSSM superpotential is given by

$$\mathcal{W} = \mathcal{W}_{RPC} + \mathcal{W}_{RPV}. \quad (1.2)$$

Here \mathcal{W}_{RPC} is the superpotential in the RPC case, and \mathcal{W}_{RPV} is the RPV superpotential given by

$$\begin{aligned} \mathcal{W}_{RPC} &= (Y_E)_{ij} H_d L_i \bar{E}_j + (Y_D)_{ij} H_d Q_i \bar{D}_j + (Y_U)_{ij} Q_i H_u \bar{U}_j - \mu H_d H_u, \\ \mathcal{W}_{RPV} &= \frac{1}{2} \lambda_{ijk} L_i L_j \bar{E}_k + \lambda'_{ijk} L_i Q_j \bar{D}_k - \mu_i L_i H_u, \end{aligned} \quad (1.3)$$

where we have suppressed all gauge indices, and baryon-number violating terms of the form $\lambda''_{ijk} \bar{U}_i \bar{D}_j \bar{D}_k$ are forbidden by baryon triality. The $\{i, j, k\} \in \{1, 2, 3\}$ are family indices. (Y_E) , (Y_D) and (Y_U) are 3×3 matrices of dimensionless Yukawa couplings; λ_{ijk} , λ'_{ijk} are the dimensionless trilinear RPV couplings, and μ_i are dimensionful bilinear RPV parameters.

Compared with the RPC minimal supersymmetric extension to the Standard Model (RPC MSSM), the presence of additional RPV couplings leads to distinctive signatures at a collider, as well as providing possible solutions to physics problems other than the technical hierarchy problem. A prime example concerns the neutrino sector. As the RPV couplings violate lepton number by 1 and always involve lepton doublets, they automatically lead to Majorana neutrino masses [12–20] without the need to introduce additional field content, for instance a right handed neutrino. The Majorana nature of the neutrinos leads to neutrinoless double beta decay through the ‘1-1’ entry in the neutrino mass matrix $m_{\beta\beta}$ (hence we refer to this mechanism as $m_{\beta\beta}$ contribution in the remainder of the paper) which connects two electron neutrinos in a basis where the charged lepton mass matrix is diagonal. On top of that, there are higher dimensional effective operators unique to this class of models which mediate $0\nu\beta\beta$ without an $m_{\beta\beta}$ insertion. These operators are proportional to either $\lambda'_{111}\lambda'_{111}$ or $\lambda'_{113}\lambda'_{131}$, of which the detailed quark level processes and relevant nuclear matrix element calculations involved were discussed in [1, 2] and [3–5] respectively. In principle, the product $\lambda'_{112}\lambda'_{121}$ could also lead to $0\nu\beta\beta$. However, this coupling product is tightly constrained by K^0 - \bar{K}^0 mixing [21], and hence this contribution is neglected in the rest of this paper. The bilinear operators could also lead to direct $0\nu\beta\beta$. As discussed in [22], bilinear neutrino mass terms consistent with the observed neutrino mass scales typically lead to a negligible contribution to the $0\nu\beta\beta$ rate, so their

contributions will also not be discussed further. The quark level processes for $\lambda'_{111}\lambda'_{111}$ and $\lambda'_{113}\lambda'_{131}$ will be discussed in more detail later. As these operators violate lepton number by two units without the need of an $m_{\beta\beta}$ insertion, they are not suppressed by the smallness of the neutrino masses as a result. These channels will be called *direct contribution* from here-on. On the other hand, the couplings responsible for direct contribution also generate neutrino masses and thus $m_{\beta\beta}$, as these couplings necessarily violate electron number. In general these different processes can contribute to $0\nu\beta\beta$ simultaneously, so depending on the magnitude of such contributions, interference between the direct and $m_{\beta\beta}$ decay matrix elements may be important in determining the decay rate of $0\nu\beta\beta$ in this class of models.

In this paper we concentrate on constraints from heavy flavour physics and the Large Hadron Collider (LHC) that provide indirect information on possible $0\nu\beta\beta$ mechanisms in the RPV MSSM. First, the $0\nu\beta\beta$ bound on the direct contribution mediated by the coupling product $\lambda'_{113}\lambda'_{131}$ depends on the two sbottom masses. The same coupling product is also constrained by B_d^0 - \bar{B}_d^0 mixing [4, 21, 23], with the bound being dependent on the electron sneutrino mass. Knowledge of the masses of the electron sneutrino and that of the sbottoms will therefore allow us to infer whether this direct contribution mechanism could be the dominant source of $0\nu\beta\beta$. Second, the direct contribution mediated by λ'_{111} also leads to single selectron production at hadron colliders (see [24–30] for an analysis on the related process of single smuon production and the associated bound). Even though there exist stringent bounds on the product $\lambda'_{111}\lambda'_{111}$ [1, 2, 31, 32] from non-observation of $0\nu\beta\beta$ for a low SUSY mass scale of around 100 GeV, its strong dependence on the SUSY mass scale means that this bound relaxes rapidly as one raises the SUSY scale, making single selectron production at the LHC potentially observable for heavier mass spectra.

In the presence of R-parity violation, one cannot infer unambiguously the value of $m_{\beta\beta}$ from the lower bound on $0\nu\beta\beta$ half-life $T_{1/2}^{0\nu\beta\beta}$. Nevertheless, since the RPV couplings in turn generate neutrino masses, knowledge of the magnitude of the relevant RPV coupling could still allow us to obtain information on $m_{\beta\beta}$ and hence the possible neutrino mass spectrum. The aim of this paper is to explore the interplay between the RPV effects mentioned above, in particular how different constraints and observations may shed light on the underlying mechanism of $0\nu\beta\beta$. A first exploration on the relationship between $0\nu\beta\beta$ decay rate and single slepton production at the LHC may be found in [33]. A complementary way to probe mechanisms of $0\nu\beta\beta$ was discussed in [34, 35] by combining measurements from different nuclei.

For concreteness, we only consider $0\nu\beta\beta$ of ^{76}Ge . In the rest of this paper, numerical values of nuclear matrix elements (NMEs) and half life all refer to this nuclei. We shall also restrict ourselves to mass spectra with minimal supergravity (mSUGRA) assumption. A related work on contributions of trilinear RPV terms to $0\nu\beta\beta$ in GUT constrained MSSM scenario is presented in [36]. There, particular attention is paid to nuclear matrix element calculations and contributions from different sparticles in the presence of a non-zero λ'_{111} coupling. In our present work, while we specify GUT constrained mass spectra, the bounds on the RPV couplings are computed at the SUSY scale. We also include a discussion on $\lambda'_{113}\lambda'_{131}$, and focus mainly on the interplay between different experimental measurements and the implications of these results for $0\nu\beta\beta$.

This paper is organised as follows. In section 2 we briefly review the possible $0\nu\beta\beta$ mechanisms in the RPV MSSM, and discuss the quark level matrix elements calculated in the literature. The current experimental half life limit $T_{1/2}^{0\nu\beta\beta}$ of ^{76}Ge , as well as the neutrino oscillation data are summarised in section 3. We also list some useful scaling relations between the RPV parameter bounds and SUSY breaking parameters and the values of the NMEs (see [37,38] for reviews) used there. In section 4 we proceed to discuss how the RPV contribution to $B_d^0-\bar{B}_d^0$ mixing can affect the possibility of $\lambda'_{113}\lambda'_{131}$ direct contribution to be the dominant observable $0\nu\beta\beta$ channel. Finally, we investigate the prospects of observing the single selectron resonance at the LHC and its implication of $0\nu\beta\beta$ in section 5 before our concluding remarks.

2. Mechanisms of $0\nu\beta\beta$ in the RPV MSSM

In the RPV MSSM, it is possible to construct neutrino mass models that explain the neutrino oscillation data. This also means that the standard light Majorana neutrino exchange with a mass insertion $m_{\beta\beta}$ is present. In addition, there are direct channels via coupling products proportional to $\lambda'_{113}\lambda'_{131}$ and $\lambda'_{111}\lambda'_{111}$.

We assume that the neutrino masses, hence $m_{\beta\beta}$, are generated entirely from the trilinear RPV couplings, and do not introduce additional fields such as heavy right handed neutrinos or Higgs triplets, as in type I [39] and type II [40,41] see-saw models respectively, nor introduce non-zero bilinear RPV couplings. For a realistic model, one expects there to be many non-vanishing RPV operators present in order to fill out the effective 3×3 neutrino mass matrix with non-zero entries. These operators could have consequences for collider searches of single selectron production, which will be discussed later.

2.1 Light Majorana neutrino exchange: $0\nu\beta\beta$ via $m_{\beta\beta}$

The RPV coupling products $\lambda'_{ilm}\lambda'_{jml}$ contribute to the neutrino mass matrix $(m_\nu)_{ij}$, in particular the ‘1-1’ entry $m_{\beta\beta}$. A Feynman diagram using the mass insertion approximation (MIA) [42] with $\lambda'_{113}\lambda'_{131}$ is shown in fig. 1.

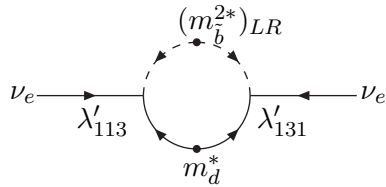


Figure 1: A MIA diagram showing contribution of $m_{\beta\beta}$ from the product $\lambda'_{113}\lambda'_{131}$.

An expression which corresponds to fig. 1 in the MIA is given by

$$m_{\beta\beta} \simeq \frac{3m_d}{8\pi^2} \frac{\lambda'_{113}\lambda'_{131}m_{bLR}^2}{m_{bLL}^2 - m_{bRR}^2} \ln\left(\frac{m_{bLL}^2}{m_{bRR}^2}\right) + (b \leftrightarrow d). \quad (2.1)$$

Here $m_{b_{LL}}^2$, $m_{b_{RR}}^2$ and $m_{b_{LR}}^2$ represents the entries of the sbottom mass matrix in an obvious notation, and m_d is the running mass of the down quark. As is well-known, $0\nu\beta\beta$ proceeds via exchange of a virtual Majorana neutrino with a $m_{\beta\beta}$ insertion. We shall not elaborate any further except for stating the effective Lagrangian after integrating out the W gauge boson, and the $\Delta L_e = 2$ Lagrangian with a virtual Majorana neutrino as follows

$$\begin{aligned}\mathcal{L}_{EW}^{eff}(x) &= -\frac{G_F}{\sqrt{2}} \left[\bar{e} \gamma^\mu (1 - \gamma_5) \nu \bar{u}_y \gamma_\mu (1 - \gamma_5) d^y \right], \\ \mathcal{L}_{EW}^{eff, \Delta L_e=2}(x) &= \frac{G_F^2}{2} \left[\bar{e} \gamma_\mu (1 - \gamma_5) \frac{m_{\beta\beta}}{q^2} \gamma_\nu e^c \right] \left[J_{V-A}^\mu J_{V-A}^\nu \right],\end{aligned}\quad (2.2)$$

where y is a colour index, and in the second line of eq. (2.2), $J_{V-A}^\mu = \bar{u}_y \gamma^\mu (1 - \gamma_5) d^y$. A Feynman diagram depicting this process is displayed in fig. 2.

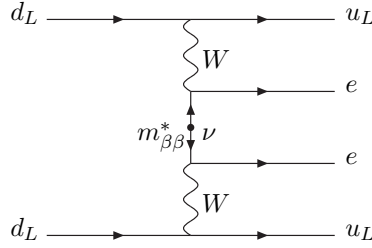


Figure 2: A Feynman diagram showing $0\nu\beta\beta$ via exchange of a virtual Majorana neutrino.

2.2 Heavy sbottom exchange: $0\nu\beta\beta$ via $\lambda'_{113}\lambda'_{131}$

In the basis where both the down-type quark and the charged lepton mass matrices are diagonal, the coupling product $\lambda'_{113}\lambda'_{131}$ leads to an effective Lagrangian involving exchange of one SUSY particle of the form

$$\begin{aligned}\mathcal{L}_{\lambda'_{113}\lambda'_{131}}^{eff}(x) &= \frac{G_F}{8\sqrt{2}} \eta^n (U_{PMNS}^*)_{ni} \left[\frac{1}{2} (\bar{\nu}_i \sigma^{\mu\nu} (1 + \gamma_5) e^c) (\bar{u}_y \sigma_{\mu\nu} (1 + \gamma_5) d^y) \right. \\ &\quad \left. + 2(\bar{\nu}_i (1 + \gamma_5) e^c) (\bar{u}_z (1 + \gamma_5) d^z) \right],\end{aligned}\quad (2.3)$$

where

$$\begin{aligned}
\eta^n &= \sum_k \frac{\lambda'_{1mk} \lambda'_{nk1} (U_{CKM})_{1m}}{2\sqrt{2}G_F} \sin 2\theta_{\tilde{d}_k} \left(\frac{1}{m_{\tilde{d}_k(1)}^2} - \frac{1}{m_{\tilde{d}_k(2)}^2} \right) \\
&= - \sum_k \frac{\lambda'_{1mk} \lambda'_{nk1} (U_{CKM})_{1m}}{\sqrt{2}G_F} \left(\frac{m_{\tilde{d}_k(LR)}^2}{m_{\tilde{d}_k(LL)}^2 m_{\tilde{d}_k(RR)}^2 - m_{\tilde{d}_k(LR)}^4} \right) \\
&\simeq \frac{\lambda'_{113} \lambda'_{n31}}{2\sqrt{2}G_F} \sin 2\theta_{\tilde{b}} \left(\frac{1}{m_{\tilde{b}_1}^2} - \frac{1}{m_{\tilde{b}_2}^2} \right) \\
&= - \frac{\lambda'_{113} \lambda'_{n31}}{\sqrt{2}G_F} \left(\frac{m_{\tilde{b}_{LR}}^2}{m_{\tilde{b}_{LL}}^2 m_{\tilde{b}_{RR}}^2 - m_{\tilde{b}_{LR}}^4} \right). \tag{2.4}
\end{aligned}$$

In the above Lagrangian, U_{PMNS} is the 3×3 unitary PMNS neutrino mixing matrix [43,44], and $\sigma^{\mu\nu} = \frac{i}{2}[\gamma^\mu, \gamma^\nu]$. Note that the factor of $\frac{1}{2}$ in the first term of eq. (2.3) is absent in [4, 5]. However, our calculation agrees with the *published* version of [45]. In eq. (2.4), U_{CKM} is the CKM matrix in the quark sector, and $m_{\tilde{d}_k(LL,LR,RR)}^2$ denote entries in the k -th generation down type squark mass squared matrix. In particular, $m_{\tilde{b}_1}$ and $m_{\tilde{b}_2}$ denote the 2 sbottom mass eigenvalues, and $\theta_{\tilde{b}}$ is the sbottom left-right mixing angle. The relations between the mixing angle and the entries in the mass and flavour basis sbottom mass matrices follow those in SOFTSUSY [46]. The corresponding expressions in terms of mass insertion in flavour basis are also displayed. The chirality structure of the scalar exchange together with the form of the RPV couplings result in a left handed out-going neutrino, as opposed to a right handed out-going (anti) neutrino as in the $m_{\beta\beta}$ mechanism. As a result, the complete $0\nu\beta\beta$ matrix element with a leptonic current coupled to a quark current via a W boson does not contain a neutrino mass insertion, and hence is not suppressed by the light neutrino mass scale. The $\Delta L_e = 2$ Lagrangian is given by

$$\begin{aligned}
\mathcal{L}_{EW+\lambda'_{113}\lambda'_{131}}^{eff, \Delta L_e=2}(x) &= \frac{G_F^2}{2} \eta^1 \left[\frac{1}{2} \left(\bar{e} \gamma_\rho (1 - \gamma_5) \frac{1}{\not{q}} e^c \right) J_{V-A}^\rho J_{PS} \right. \\
&\quad \left. + \frac{1}{8} \left(\bar{e} \gamma_\rho (1 - \gamma_5) \frac{1}{\not{q}} \sigma_{\mu\nu} e^c \right) J_{V-A}^\rho J_T^{\mu\nu} \right], \tag{2.5}
\end{aligned}$$

where $J_{PS} = \bar{u}_y(1 + \gamma_5)d^y$ and $J_T^{\mu\nu} = \bar{u}_y\sigma^{\mu\nu}(1 + \gamma_5)d^y$ are the pseudo-scalar and tensor currents respectively. A Feynman diagram depicting this process is displayed in fig. 3.

It should be noted that $\lambda'_{111}\lambda'_{111}$ can also mediate $0\nu\beta\beta$ via a diagram similar to fig. 3. However, in the case of $\lambda'_{111}\lambda'_{111}$, there are other diagrams contributing to $0\nu\beta\beta$ (but not for $\lambda'_{113}\lambda'_{131}$). These contributions dominate over the one described in this subsection, and will be discussed next.

2.3 Heavy sparticle exchange: $0\nu\beta\beta$ via $\lambda'_{111}\lambda'_{111}$

Following the notation of [1], the effective Lagrangian with λ'_{111} in the direct RPV $0\nu\beta\beta$ process involving exchange of two SUSY particles is given by

$$\begin{aligned}
\mathcal{L}_{\lambda'_{111}\lambda'_{111}}^{eff, \Delta L_e=2}(x) &= \frac{G_F^2}{2} m_p^{-1} [\bar{e}(1 + \gamma_5)e^c] \\
&\quad \times \left[(\eta_{\tilde{g}} + \eta_\chi)(J_{PS}J_{PS} - \frac{1}{4}J_T^{\mu\nu}J_{T\mu\nu}) + (\eta_{\chi\tilde{e}} + \eta'_{\tilde{g}} + \eta_{\chi\tilde{f}})J_{PS}J_{PS} \right], \tag{2.6}
\end{aligned}$$

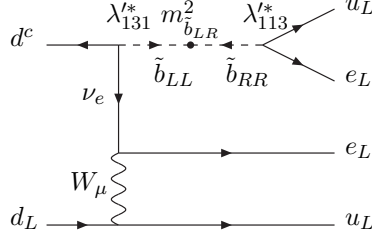


Figure 3: Direct $\lambda'_{113}\lambda'_{131}$ contribution to $0\nu\beta\beta$.

where the RPV coefficients are defined to be

$$\begin{aligned}
\eta_{\tilde{g}} &= \frac{\pi\alpha_s}{6} \frac{\lambda_{111}^{\prime 2}}{G_F^2} \frac{m_p}{m_{\tilde{g}}} \left(\frac{1}{m_{\tilde{u}_L}^4} + \frac{1}{m_{\tilde{d}_R}^4} - \frac{1}{2m_{\tilde{u}_L}^2 m_{\tilde{d}_R}^2} \right), \\
\eta_{\chi} &= \frac{\pi\alpha_2}{2} \frac{\lambda_{111}^{\prime 2}}{G_F^2} \sum_{i=1}^4 \frac{m_p}{m_{\chi_i}} \left(\frac{\epsilon_{L_i}^2(u)}{m_{\tilde{u}_L}^4} + \frac{\epsilon_{R_i}^2(d)}{m_{\tilde{d}_R}^4} - \frac{\epsilon_{L_i}(u)\epsilon_{R_i}(d)}{m_{\tilde{u}_L}^2 m_{\tilde{d}_R}^2} \right), \\
\eta_{\chi\tilde{e}} &= 2\pi\alpha_2 \frac{\lambda_{111}^{\prime 2}}{G_F^2} \sum_{i=1}^4 \frac{m_p}{m_{\chi_i}} \left(\frac{\epsilon_{L_i}^2(e)}{m_{\tilde{e}_L}^4} \right), \\
\eta'_{\tilde{g}} &= \frac{2\pi\alpha_s}{3} \frac{\lambda_{111}^{\prime 2}}{G_F^2} \frac{m_p}{m_{\tilde{g}}} \left(\frac{1}{m_{\tilde{u}_L}^2 m_{\tilde{d}_R}^2} \right), \\
\eta_{\chi\tilde{f}} &= \pi\alpha_2 \frac{\lambda_{111}^{\prime 2}}{G_F^2} \sum_{i=1}^4 \frac{m_p}{m_{\chi_i}} \left(\frac{\epsilon_{L_i}(u)\epsilon_{R_i}(d)}{m_{\tilde{u}_L}^2 m_{\tilde{d}_R}^2} - \frac{\epsilon_{L_i}(u)\epsilon_{L_i}(e)}{m_{\tilde{u}_L}^2 m_{\tilde{e}_L}^2} - \frac{\epsilon_{L_i}(e)\epsilon_{R_i}(d)}{m_{\tilde{e}_L}^2 m_{\tilde{d}_R}^2} \right), \quad (2.7)
\end{aligned}$$

and again we follow the notation of [1]. In particular the ϵ 's denote rotations between mass and gauge eigenbasis in the gaugino-fermion-sfermion vertices. To facilitate comparisons with the literature, we display only the first generation sparticle contribution above but include contributions from all three generations in the numerical calculations. The relevant Feynman diagrams are displayed in fig. 4.

Note that our expressions above are different from those presented in [1], [2] and [47]. The former reference made an approximation when extracting the colour singlet currents from the Feynman diagrams. Also, the expressions for η_{χ} and $\eta_{\chi\tilde{f}}$ (following the convention of [1]) are different, with the discrepancy coming from the colour flows of fig. 4(e) and fig. 4(f). The latter two references took proper account of the colour singlet extraction, which we have checked independently. However they have left η_{χ} and $\eta_{\chi\tilde{f}}$ in the same form as [1]. The numerical differences between the references and our results are however small compared with the uncertainty in the nuclear matrix elements, at least in the parameter space we explore.

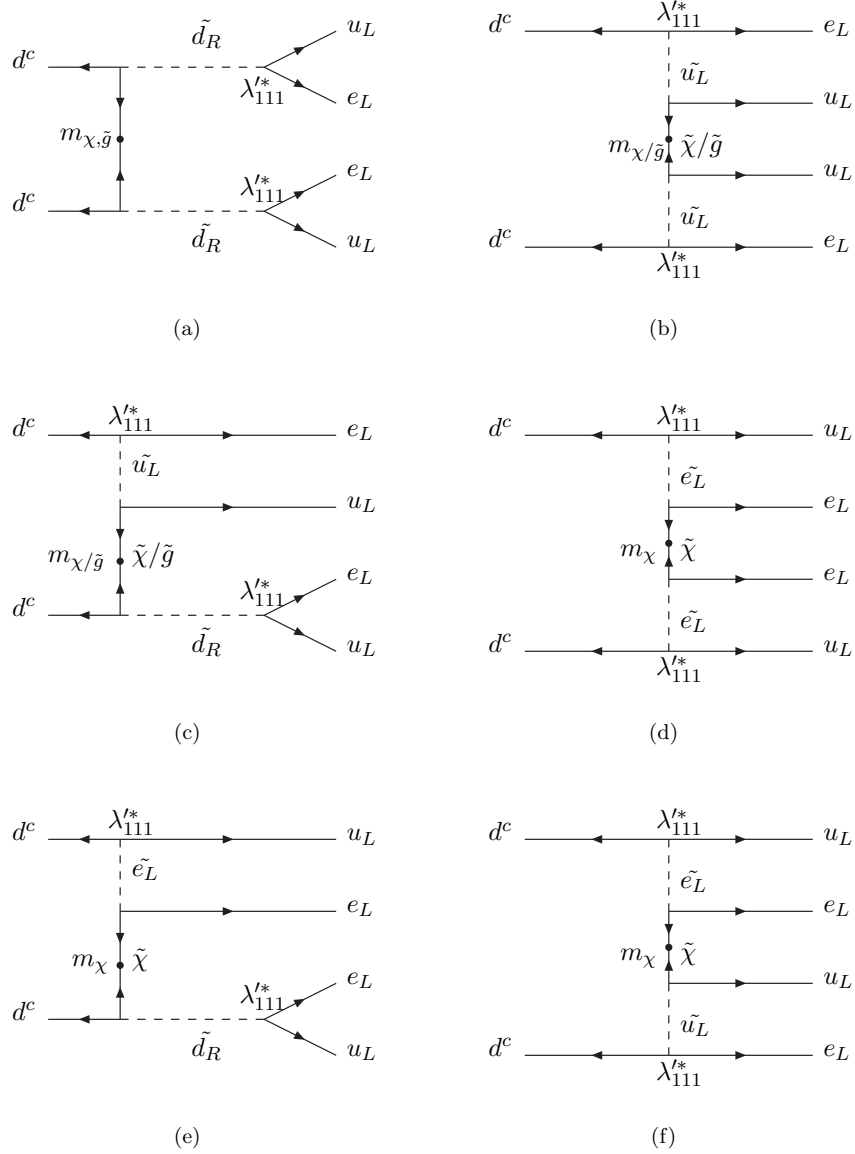


Figure 4: $\lambda'_{111}\lambda'_{111}$ contributions to $0\nu\beta\beta$.

3. Experimental limits and nuclear matrix elements

The most stringent lower limit on the ^{76}Ge $0\nu\beta\beta$ half life was measured in the Heidelberg-Moscow experiment [48, 49] to be

$$T_{1/2}^{0\nu\beta\beta} \geq 1.9 \cdot 10^{25} \text{ yrs.} \quad (3.1)$$

Depending on the RPV couplings considered, different mechanisms dominate the $0\nu\beta\beta$ process. Thus the above limit can be translated to upper bounds on particular products

of RPV couplings. For the model under consideration, the relevant formulae are given by

$$\begin{aligned} (T_{1/2}^{0\nu\beta\beta})^{-1} &= G_{01} \left| -M_{\lambda'_{113}\lambda'_{131}} + \frac{m_{\beta\beta}}{m_e} M_\nu \right|^2, \\ (T_{1/2}^{0\nu\beta\beta})^{-1} &= G_{01} \left| M_{\lambda'_{111}} \right|^2, \end{aligned} \quad (3.2)$$

where $G_{01} = 7.93 \cdot 10^{-15} \text{yr}^{-1}$ [50] is a precisely calculable phase space factor. The M_i for $i = \{\lambda'_{111}, \lambda'_{113}\lambda'_{131}, \nu\}$ denote matrix elements from different contributions including effects from both the quark and the nucleon levels. These contributions are given by

$$M_{\lambda'_{113}\lambda'_{131}} = \eta^1 M_q^{2N}, \quad (3.3)$$

$$\begin{aligned} M_{\lambda'_{111}} &= (\eta_{\bar{g}} + \eta_\chi) M_{\bar{g}}^{2N} + (\eta_{\chi\bar{e}} + \eta'_{\bar{g}} + \eta_{\chi\bar{f}}) M_f^{2N} \\ &\quad + \frac{3}{8} \left((\eta_{\bar{g}} + \eta_\chi) + \frac{5}{3} (\eta_{\bar{g}} + \eta_\chi + \eta_{\chi\bar{e}} + \eta'_{\bar{g}} + \eta_{\chi\bar{f}}) \right) \left(\frac{4}{3} M^{1\pi} + M^{2\pi} \right), \end{aligned} \quad (3.4)$$

$$M_\nu = -\frac{M_\nu^F}{g_A^2} + M_\nu^{GT} + M_\nu^T. \quad (3.5)$$

The 3 matrix element definitions are obtained from [4], [1, 2] and [51] respectively. In the first expression, η^1 is defined as in eq. (2.4) with $n = 1$, whereas in the second expression, the η_i 's are defined as in eq. (2.7). In the nuclear matrix elements $M_{\lambda'_{113}\lambda'_{131}}$ and $M_{\lambda'_{111}}$, the superscripts $2N$, 1π and 2π denote 2 nucleon leptonic decay, 1 pion and 2 pion exchange modes, respectively. In the third expression, F , GT and T denote the Fermi, Gamow-Teller and tensor components of M_ν . The first formula in eq. (3.2) should be used in the presence of $\lambda'_{113}\lambda'_{131}$, and the relative sign between the direct and $m_{\beta\beta}$ contributions is chosen such that numerical values of the nuclear matrix elements correspond directly to those presented in [5] and [51]. The second expression in eq. (3.2) is applicable in the presence of λ'_{111} . We have neglected the $m_{\beta\beta}$ contribution in this case, which will be justified shortly. Recently, [5] has also calculated the contribution from the pion mode to $M_{\lambda'_{113}\lambda'_{131}}$ as well as an additional vector-tensor current contribution to the nucleon mode. The full nuclear matrix element (NME) is then given by

$$M_{\lambda'_{113}\lambda'_{131}} = \eta^1 (M_{\bar{q}}^{2N} + M_{\bar{q}}^\pi). \quad (3.6)$$

In this paper, we are primarily interested in collider effects due to couplings from direct contributions rather than detailed calculation of nuclear matrix elements. We adopt numerical values collected from various sources in the literature for our discussions here.² These parameters are displayed in table 1.

A breakdown of the nuclear matrix element for $\lambda'_{113}\lambda'_{131}$ displayed in table 1 is shown in table 2. In this table, $M_{\bar{q}}^{AP}$, $M_{\bar{q}}^{MT}$ and $M_{\bar{q}}^{VT}$ are the *axial vector-pseudo scalar*, *magnetic-tensor* and *vector-tensor* contributions respectively, and $M_{\bar{q}}^{2N}$ is the sum of these terms.

²The spread of different NME calculations may to some extent represent the modelling uncertainties. A glance of results tabulated in [52] suggests a factor of 3 variation for M_ν , while some of the models are obviously outdated. However in some cases, for example the 2 pion mode for direct contribution, it is difficult to use this as an order of magnitude estimate of its uncertainty due to a lack of independent calculations. A more optimistic estimate of the NME uncertainty to be only 30% has been advocated in [53].

channel	NME(^{76}Ge)	value	Ref.
$\lambda'_{111}\lambda'_{111}$	$M_{\tilde{g}}^{2N}$	283	[1]
	$M_{\tilde{f}}^{2N}$	13.2	[1]
	$M^{1\pi}$	-18.2	[2]
	$M^{2\pi}$	-601	[2]
$\lambda'_{113}\lambda'_{131}$	$M_{\tilde{q}}^{2N}$	-0.9	[5]
	$M_{\tilde{q}}^{\pi}$	604	[5]
$m_{\beta\beta}$	M_{ν}	2.8	[51]

Table 1: Nuclear matrix elements of ^{76}Ge used. For model details of the NME calculations, we refer readers to the literature.

The values of $M_{\tilde{q}}^{MT}$ and $M_{\tilde{q}}^{VT}$ are corrected by factors of $\frac{1}{2}$ associated with the tensor current in eq. (2.3) discussed before, with the values from the original reference shown in parenthesis for ease of reference. We see that there is a strong cancellation among the nucleon modes, so the obtained value of $M_{\tilde{q}}^{2N} = -0.9$ might be subjected to significant theory uncertainty. However, this uncertainty is expected to be subdominant compared to the pion mode contribution.

Ref.	$M_{\tilde{q}}^{AP}$	$M_{\tilde{q}}^{MT}$	$M_{\tilde{q}}^{VT}$	$M_{\tilde{q}}^{2N}$	$M_{\tilde{q}}^{\pi}$
[5]	29.6(29.6)	-123(-246)	92.5(185)	-0.9(-31.4)	604(604)

Table 2: Breakdown of NME in heavy sbottom exchange used in this paper. The extra factor of $\frac{1}{2}$ from Fierz rearrangement is included. The numbers in parenthesis are obtained from the original literature.

If $m_{\beta\beta}$ is the dominant contribution to $0\nu\beta\beta$, the bound on $T_{1/2}^{0\nu\beta\beta}$ using $M_{\nu} = 2.8$ from table 1 can be translated into the limit

$$m_{\beta\beta} \lesssim 460 \text{ meV} \quad (3.7)$$

for eq. (3.1), with significant variation depending on the nuclear physics model used as discussed before. A scaling relationship between a measured half-life limit and $m_{\beta\beta}$ is given by

$$\frac{m_{\beta\beta}(\text{max})}{460\text{meV}} \simeq \left(\frac{1.9 \cdot 10^{25}\text{yr}}{T_{1/2}^{0\nu\beta\beta}(\text{min})} \right)^{1/2}. \quad (3.8)$$

If the direct contributions are instead dominant, then assuming the $m_{\beta\beta}$ contributions are negligible, for a ^{76}Ge half-life limit of $1.9 \cdot 10^{25}$ yrs, the bound on $\lambda'_{113}\lambda'_{131}$ and λ'_{111} are given by

$$\lambda'_{113}\lambda'_{131} \lesssim 2 \cdot 10^{-8} \left(\frac{\Lambda_{SUSY}}{100\text{GeV}} \right)^3, \quad (3.9)$$

$$\lambda'_{111} \lesssim 5 \cdot 10^{-4} \left(\frac{m_{\tilde{f}}}{100\text{GeV}} \right)^2 \left(\frac{m_{\tilde{g}/\tilde{\chi}}}{100\text{GeV}} \right)^{1/2} \quad (3.10)$$

from [4,5] and [1,2] respectively, after taking into account the modifications to the effective Lagrangians discussed in section 2. Here Λ_{SUSY} is an effective SUSY breaking scale for

the soft terms involved in eq. (2.4), and $m_{\tilde{f}}$ and $m_{\tilde{g}/\tilde{\chi}}$ are sfermions and gluino/neutralino masses in the dominant Feynman diagrams.

When interference between direct RPV and $m_{\beta\beta}$ contributions is small, the scaling between the measured half life and the RPV couplings is given by

$$\lambda'_{11i}\lambda'_{i11} \propto (T_{1/2}^{0\nu\beta\beta})^{-1/2}, \quad \text{no sum, } i \in \{1, 3\} \quad (3.11)$$

whether either $m_{\beta\beta}$ or direct RPV contributions dominate $0\nu\beta\beta$ decay. The above relationship between the bounds on direct couplings with the SUSY scale should be compared with the corresponding expression for (a fixed) $m_{\beta\beta}$ in eq. (2.1). For fixed RPV couplings, $M_{\lambda'_{111}}$ scales as $\Lambda_{\text{SUSY}}^{-5}$, $M_{\lambda'_{113}\lambda'_{131}}$ scales as $\Lambda_{\text{SUSY}}^{-3}$, whereas $m_{\beta\beta}$ scales as $\Lambda_{\text{SUSY}}^{-1}$. Thus the $m_{\beta\beta}$ contributions would dominate at high enough SUSY breaking scales Λ_{SUSY} . Interference between different $0\nu\beta\beta$ amplitudes could become significant even if there are no additional contributions to $m_{\beta\beta}$ other than from those responsible for direct contribution, and the above scaling relationship between the direct RPV coupling bounds and the measured $T_{1/2}^{0\nu\beta\beta}$ needs to be modified.

To illustrate this point, as well as for the analysis of the interplay among B-physics, single slepton production and $0\nu\beta\beta$, we restrict ourselves to a $A_0 = 0$ region in minimal supergravity (mSUGRA), in which flavour changing neutral currents and CP violation are typically suppressed sufficiently to conform with experimental constraints. The parameter space we choose is such that comparison with single slepton discovery reach from [24] can be made easily.

Specifically, the following set of RPC parameters are defined:

$$\begin{aligned} M_0 &= [40, 1000] \text{ GeV}, & M_{1/2} &= [40, 1000] \text{ GeV}, & A_0 &= 0, \\ \tan\beta &= 10, & \text{sgn}\mu &= +1, \end{aligned} \quad (3.12)$$

where m_0 , m_{12} and A_0 are the universal scalar, gaugino, and trilinear soft SUSY breaking parameters defined at a unification scale $M_X \sim 2.0 \cdot 10^{16} \text{ GeV}$, $\tan\beta$ is the ratio of the Higgs vacuum expectation values v_u/v_d , and $\text{sgn}\mu$ is the sign of the bilinear Higgs parameter in the superpotential.

We show in fig. 5 the square of the ratio of the matrix element contributions from direct and $m_{\beta\beta}$ diagrams, assuming the presence of only $\lambda'_{111}\lambda'_{111}$ and $\lambda'_{113}\lambda'_{131}$ in the RPV sector. The region in black at low $M_{1/2}$ has no electroweak symmetry breaking (EWSB) or the lightest Higgs mass is in violation of the LEP2 limit [54]. We have used 111.4 GeV to include a 3 GeV theory uncertainty in SOFTSUSY on the calculation of the Higgs mass, rather than 114.4 GeV, the LEP2 95% confidence level upper bound. The black contours separate regions with a neutralino LSP from those with a stau LSP. Note that in plotting this ratio, the RPV couplings drop out. It can be seen that interference between these two types of diagrams may be neglected for $\lambda'_{111}\lambda'_{111}$, where the ratio of the NMEs is greater than 20 in the region we have plotted. However for $\lambda'_{113}\lambda'_{131}$, the ratio of these two contributions can be much smaller. Depending on the choice of NMEs (recall footnote 2), interference effects could be significant. This is especially important in the $M_{1/2} \sim 1 \text{ TeV}$

region. It is also necessary to keep the sign of $m_{\beta\beta}$,³ without taking the absolute value. By comparing eq. (2.1) and eq. (2.4), we see that if M_ν and $M_{\lambda'_{113}\lambda'_{131}}$ have the same sign, there will be constructive interference between these two contributions, therefore leading to more stringent $\lambda'_{113}\lambda'_{131}$ bounds from $0\nu\beta\beta$ than when interference effects are neglected.

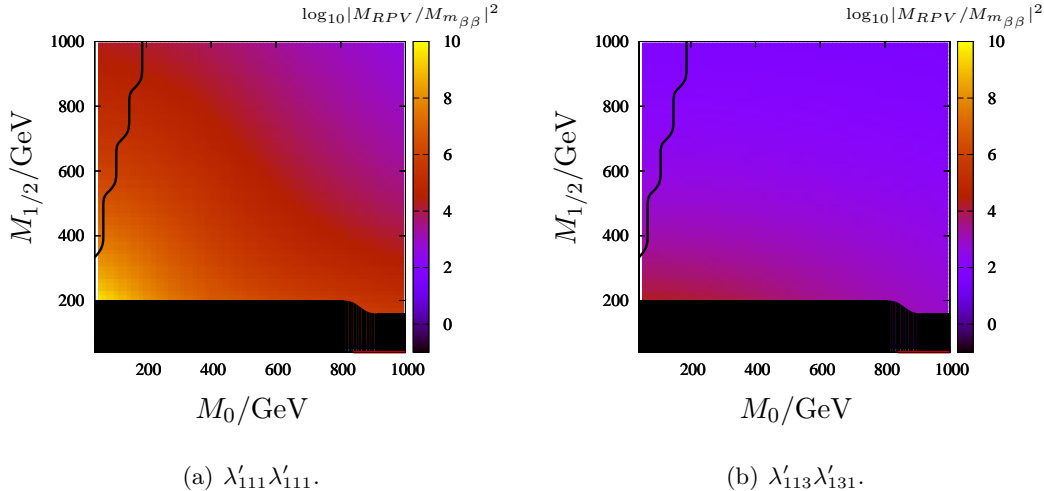


Figure 5: Comparison of direct RPV and RPV-induced $m_{\beta\beta}$ contributions to neutrinoless double beta decay, in a $M_0 - M_{1/2}$ mSUGRA parameter space with $A_0 = 0$ and $\tan\beta = 10$. Shown is the ratio of the matrix elements squared, assuming either the $\lambda'_{111}\lambda'_{111}$ or the $\lambda'_{113}\lambda'_{131}$ mechanism to be dominating. The black region at the bottom ($m_{12} \lesssim 200$ GeV) corresponds to an excluded region with either no electroweak symmetry breaking or the Higgs mass being too light. The black line in the left separates the region with a stau (to the left) and a neutralino (to the right) LSP. As can be seen from panel a), the $\lambda'_{111}\lambda'_{111}$ contribution is always dominant compared to the induced $m_{\beta\beta}$ contribution. In panel b) the ratio of direct $\lambda'_{113}\lambda'_{131}$ and induced $m_{\beta\beta}$ contributions is much smaller. Depending on the choice of NMEs, these two contributions could be comparable.

On the other hand, in many simple models of neutrino masses, generally there are additional contributions to $m_{\beta\beta}$ due to correlations between different entries in the neutrino mass matrix. Such examples can be found, for instance in [11–13, 56–61], which attempt to account for the neutrino oscillation data using a small set of RPV couplings. A recent global fit of the neutrino oscillation data is given in [62], where the following ranges of parameters at 1σ were found

$$\begin{aligned} \Delta m_{\odot}^2 &= 7.9_{-0.28}^{+0.27} \cdot 10^{-5} \text{eV}^2, & |\Delta m_{atm}^2| &= 2.6 \pm 0.2 \cdot 10^{-3} \text{eV}^2, & (3.13) \\ \sin^2\theta_{12} &= 0.31 \pm 0.02, & \sin^2\theta_{23} &= 0.47_{-0.07}^{+0.08}, & \sin^2\theta_{13} &= 0_{-0.0}^{+0.008}. \end{aligned}$$

Here Δm_{\odot}^2 and Δm_{atm}^2 denote the mass squared differences between the three neutrinos responsible for solar and atmospheric oscillations respectively. The $\sin^2\theta_{ij}$'s represent the rotation angles characterising the PMNS matrix in the standard parameterisation [63]. However, as is well-known, depending on the neutrino mass hierarchy and the (Dirac and

³It is possible to rotate $m_{\beta\beta}$ to a positive value at the expense of introducing i 's and γ_5 's to the Feynman rules. See [55] for instance. To avoid confusion we do not adopt this procedure here.

Majorana) CP violating phases assumed, the absolute value of $m_{\beta\beta}$ can range from zero to values already excluded by current $0\nu\beta\beta$ experiments [64]. The relationship between the lightest neutrino mass and the value of $m_{\beta\beta}$ for different neutrino mass hierarchies is shown in fig. 6.

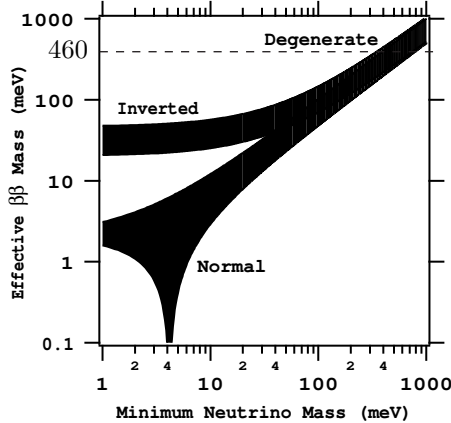


Figure 6: Value of $m_{\beta\beta}$ against the lightest neutrino mass, assuming different neutrino mass hierarchies. The figure is obtained from [52]. The dashed line corresponds to $m_{\beta\beta} = 460$ meV, the upper limit from $T_{1/2}^{0\nu\beta\beta}(^{76}\text{Ge}) = 1.9 \cdot 10^{25}$ yrs, assuming the $m_{\beta\beta}$ contribution dominates $0\nu\beta\beta$.

In the presence of direct RPV decay channels, the value of $m_{\beta\beta}$ cannot be unambiguously determined from $0\nu\beta\beta$ experiments. A signal observation in 100kg experiments no longer implies an inverted or quasi-degenerate neutrino mass spectrum, if the RPV contributions dominate $0\nu\beta\beta$. Similarly, a large $m_{\beta\beta}$ close to the cosmological limit [65]

$$\sum m_\nu \lesssim 0.7\text{eV} \quad @ 95\% \text{ CL} \quad (3.14)$$

does not necessarily lead to $0\nu\beta\beta$ at an observable rate, if the direct RPV amplitudes interfere destructively with that of $m_{\beta\beta}$. Interestingly, further information regarding the possible amplitude of the direct RPV contributions may be obtained from heavy flavour physics and from collider experiments. For the product $\lambda'_{113}\lambda'_{131}$, the combined knowledge of the masses of the electron sneutrino and sbottoms and constraints from $B_d^0-\bar{B}_d^0$ mixing could allow us to determine an upper bound on the decay amplitude $M_{\lambda'_{113}\lambda'_{131}}$. For $\lambda'_{111}\lambda'_{111}$, observation of single slepton production, for instance at the LHC, could provide valuable information on the value of λ'_{111} , which could allow further inference on the possible neutrino mass model structure consistent with (non-)observation of $0\nu\beta\beta$. In the next two sections we shall explore these two possibilities in more detail.

4. Implications of $\lambda'_{113}\lambda'_{131}$ bound from $B_d^0-\bar{B}_d^0$ on $0\nu\beta\beta$ in mSUGRA

It was shown in [4] that for sparticle masses of ~ 100 GeV, a stringent bound on $\lambda'_{113}\lambda'_{131}$ comes from $0\nu\beta\beta$. Another competing bound comes from $B_d^0-\bar{B}_d^0$ mixing. A Feynman diagram of the latter process is displayed in fig. 7.

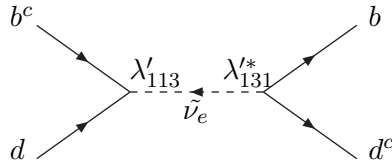
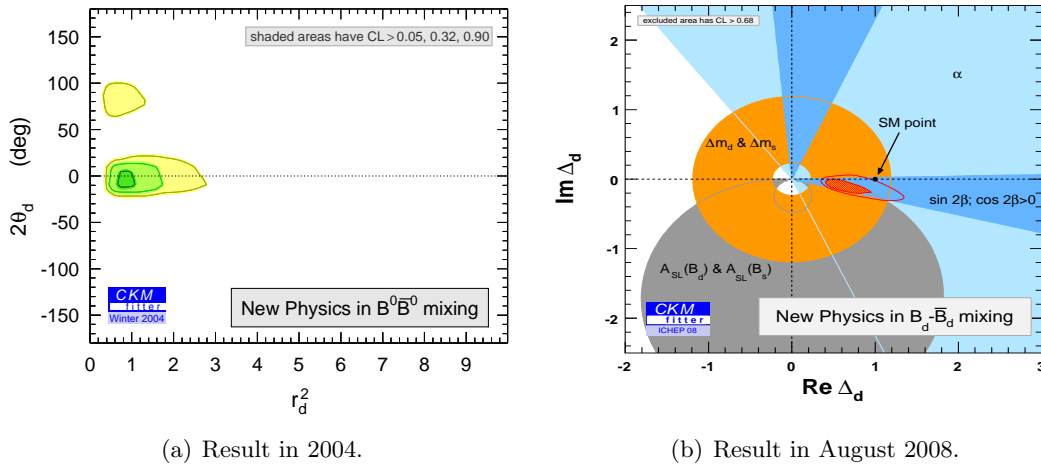


Figure 7: $B_d^0\text{-}\bar{B}_d^0$ mixing through coupling product $\lambda'_{113}\lambda'_{131}$.

An analysis by the CKMfitter Group [66] shows that while a Standard Model solution to $B_d^0\text{-}\bar{B}_d^0$ mixing is favoured, new physics effects as large as 1–2 times the SM contribution are allowed at 95% confidence level. A recent update [67] by the same group shows that again at 95% confidence level, the magnitude of any new physics effect must be less than the SM contribution. A comparison of these two results is shown in fig. 8.



(a) Result in 2004.

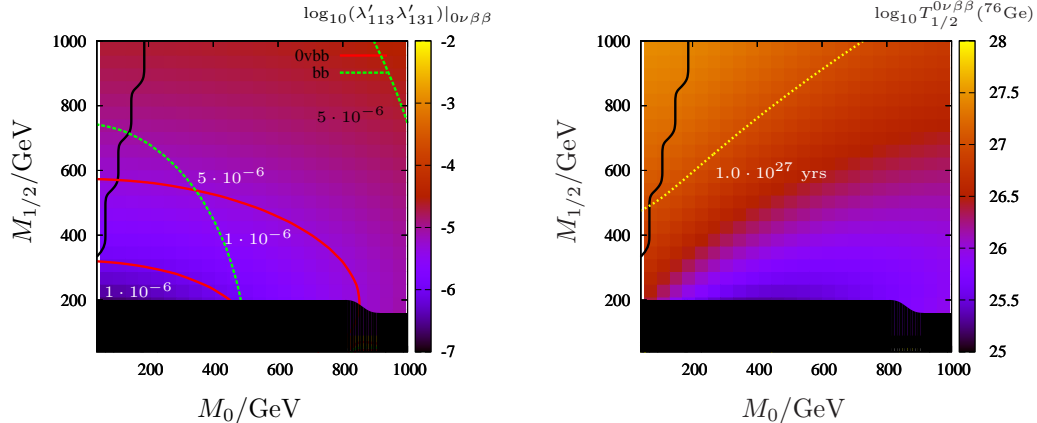
(b) Result in August 2008.

Figure 8: Change in possible new physics contributions to $B_d^0\text{-}\bar{B}_d^0$. The 95% C.L. region shown in yellow in fig. 8(a) (year 2004) is compared with the corresponding region bounded in solid orange line in fig. 8(b) (year 2008). The SM solution is located at $r_d^2 e^{i2\theta_d} = \text{Re}(\Delta_d) + \text{Im}(\Delta_d) = 1$, and deviation from the SM value may be attributed to the RPV contributions proportional to $\lambda'_{113}\lambda'_{131}$. Compared with fig. 8(a), the allowed magnitude of new physics contributions decreases by about a factor of 2 in fig. 8(b). This corresponds roughly to a factor of 4 increase in the predicted lower $T_{1/2}^{0\nu\beta\beta}$ limit.

In this figure, the two sets of axis are related to each other by

$$r_d^2 e^{i2\theta_d} - 1 = \text{Re}(\Delta_d) + \text{Im}(\Delta_d) - 1 \propto \lambda'_{113}\lambda'_{131}, \quad (4.1)$$

where the Standard Model solution is located at $r_d^2 e^{i2\theta_d} = \text{Re}(\Delta_d) + \text{Im}(\Delta_d) = 1$, and deviation from unity represents new physics effects contributing to $B_d^0\text{-}\bar{B}_d^0$ mixing. We have assumed in the above expression that all such contributions come from the sbottom exchange depicted in fig. 7. The change in upper limit of $\lambda'_{113}\lambda'_{131}$ then corresponds to a factor of 4 increase in the predicted lower $T_{1/2}^{0\nu\beta\beta}$ limit.



(a) Upper bounds from $0\nu\beta\beta$ and $B_d^0-\bar{B}_d^0$.

(b) Min $T_{1/2}^{0\nu\beta\beta}$ from $B_d^0-\bar{B}_d^0$ bound.

Figure 9: Comparison of sensitivities on $\lambda'_{113}\lambda'_{131}$ from $0\nu\beta\beta$ and from $B_d^0-\bar{B}_d^0$ in a $M_0 - M_{1/2}$ mSUGRA plane, with $A_0 = 0$ and $\tan\beta = 10$.

In 9(a) we show two sets of iso-contours with values (from the lower left) $\lambda'_{113}\lambda'_{131} = 1.0 \cdot 10^{-6}$ and $5.0 \cdot 10^{-6}$. The green dashed lines are upper bounds obtained from $B_d^0-\bar{B}_d^0$ mixing, while the solid red lines are upper bounds obtained from the experimental $T_{1/2}^{0\nu\beta\beta}(^{76}\text{Ge})$ limit of $1.9 \cdot 10^{25}$ yrs. The colour background corresponds to the $0\nu\beta\beta$ bound. The upper bounds on $\lambda'_{113}\lambda'_{131}$ from $B_d^0-\bar{B}_d^0$ are then used to calculate lower limits of $T_{1/2}^{0\nu\beta\beta}$. The results are shown in 9(b). The yellow dotted lines correspond to $T_{1/2}^{0\nu\beta\beta} = 1.0 \cdot 10^{27}$ yrs. A $T_{1/2}^{0\nu\beta\beta}$ within this range could be observable in the near future.

For our comparison with the limit from $0\nu\beta\beta$, we scale the limit from [4], which corresponds roughly to twice the size of the SM contribution, to a limit consistent with the new CKMfitter group result. This leads to

$$\lambda'_{113}\lambda'_{131} \leq 4.0 \cdot 10^{-8} \frac{m_{\tilde{\nu}_e}^2}{(100\text{GeV})^2}. \quad (4.2)$$

As we can see, this bound relaxes as the square of the sneutrino mass $m_{\tilde{\nu}_e}^2$.

To compare limits on $\lambda'_{113}\lambda'_{131}$ from $B_d^0-\bar{B}_d^0$ and from $0\nu\beta\beta$, we recall that the bound from $0\nu\beta\beta$ depends on the sbottom mass squared matrix. In the case where all SUSY breaking parameters are of the same order of magnitude, this bound relaxes as the cube of the sbottom mass scale,⁴ which is more rapid compared with the $B_d^0-\bar{B}_d^0$ bound in eq. (4.2). However in the most general MSSM the mass parameters relevant for these two bounds are independent. Which of the bounds is more stringent depends therefore on the ratio of sneutrino to sbottom masses.

In the following, we restrict our discussion to a $M_0 - M_{1/2}$ mSUGRA plane with $A_0 = 0$ and $\tan\beta = 10$. The interplay between the two sets of bounds is displayed in fig. 9. As we can see, the bound from $B_d^0-\bar{B}_d^0$ is the most stringent on the entire plane. The

⁴This is with the understanding that μ in the superpotential and $\tan\beta$ also enter the sbottom mass matrix, and can also play an important role in constraining $\lambda'_{113}\lambda'_{131}$.

bound obtained from $0\nu\beta\beta$ gets stronger for lower $M_{1/2}$, and is not particularly sensitive to variations in M_0 . This is because the sbottom masses are relatively light in this region, and their masses depend significantly on $M_{1/2}$ due to large renormalisation effects from the gluino mass. On the other hand, the sneutrino mass does not depend strongly on $M_{1/2}$. A result of this is that when moving to regions with higher $M_{1/2}$, the sbottom mass increases much faster than the sneutrino mass, hence the $0\nu\beta\beta$ bound relaxes more rapidly and the limit from $B_d^0\text{-}\bar{B}_d^0$ mixing becomes even more dominant.

The bound from $B_d^0\text{-}\bar{B}_d^0$ mixing can be used together with $M_{\lambda'_{113}\lambda'_{131}}$ to obtain a lower limit on $T_{1/2}^{0\nu\beta\beta}$, assuming contributions from $\lambda'_{113}\lambda'_{131}$ dominate this process. The result is shown in fig. 9(b). We see that $T_{1/2}^{0\nu\beta\beta} \sim 10^{26}\text{-}10^{27}$ yrs in much of the parameter space, and $0\nu\beta\beta$ can be detected by next generation experiments. In particular, there exist good prospects of observing a $0\nu\beta\beta$ signal in the region with relatively low $M_{1/2}$.

5. Single selectron production at the LHC via λ'_{111}

Depending on the value of λ'_{111} , resonant production of a single selectron may be observed at the LHC. A related process of single smuon production is studied in [24]. There, the authors rely on like-sign lepton signals to reduce the background. A diagram showing such a like-sign lepton production, with decay of a selectron via a neutralino is displayed in fig. 10. Earlier studies based on different signatures can be found in [25–29]. A first study of single slepton production in stau LSP scenarios can be found in [30]. However, to the best of our knowledge, the discovery reach of these scenarios at the LHC is not available in the literature, and hence our following discussion will be restricted to the case with a neutralino LSP.

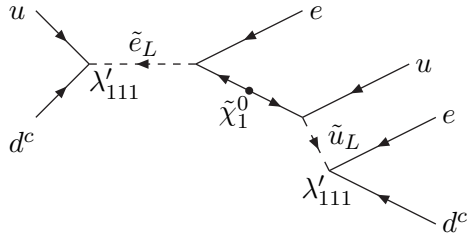


Figure 10: Production of a single selectron at resonance via λ'_{111} , followed by a gauge decay into an electron with a neutralino LSP. The LSP further decays into three final states via a virtual sparticle, leading to a same sign, di-lepton signal for the whole resonance production process. In this figure, we show only one $\tilde{\chi}$ decay diagram with a virtual up squark. The arrows represent chirality flow of left handed fermions. For the scalars, the arrows represent the would-be chirality flow of their fermion superpartners.

At low sparticle mass scales of ~ 100 GeV, the stringent bound from $0\nu\beta\beta$ renders such a process unobservable. However from eq. (3.10) the strong dependence of this bound on the SUSY mass scale implies it may be possible for single selectron production to

be observed at higher SUSY mass scales. In fig. 11, we compare the discovery reach of λ'_{211} [24] at the LHC via single smuon production with the current experimental bound on λ'_{111} coming from $0\nu\beta\beta$. As the work does not include detector effects, the reach of λ'_{211} is expected to be readily applied to λ'_{111} without significant changes. For this reason we shall use the discovery reach of λ'_{211} interchangeably with that of λ'_{111} from now on.

The study of single slepton production assumes 10fb^{-1} of data at CM energy of 14 TeV, and the analysis is performed in a $M_0 - M_{1/2}$ mSUGRA plane with $A_0 = 0$ and $\tan\beta = 10$. In fig. 11, the black/stripped regions with small $M_{1/2}$ are excluded as before,⁵ whereas the black/hatched regions with high $M_{1/2}$ and low M_0 have a stau LSP. The latter is excluded in our discussion only because the analysis in [24] assumes a neutralino LSP, while similar analysis in the case of a stau LSP is not available.

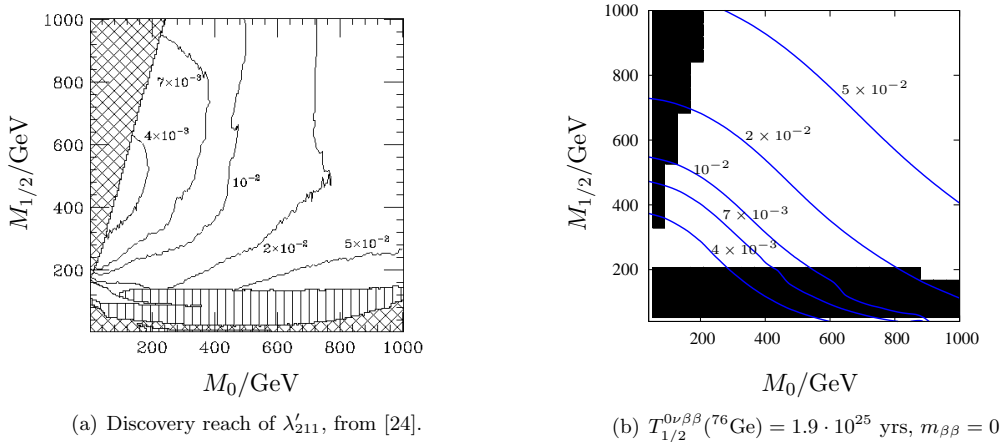


Figure 11: Comparison of the λ'_{211} discovery reach at the LHC through single slepton production with the bound on λ'_{111} from $0\nu\beta\beta$, in a $M_0 - M_{1/2}$ mSUGRA plane with $A_0 = 0$ and $\tan\beta = 10$. In fig. 11(a), the reach of λ'_{211} can readily be applied to λ'_{111} , as the collider analysis [24] did not take detector effects into account. Fig. 11(b) displays the corresponding iso-contours of λ'_{111} that lead to the current lower $T_{1/2}^{0\nu\beta\beta}({}^{76}\text{Ge})$ limit of $1.9 \cdot 10^{25}$ yrs. Here $m_{\beta\beta} = 0$ has been assumed, hence no interference between different decay mechanisms is included. As before, the black regions with small $M_{1/2}$ are ruled out. The triangular regions to the upper left have a stau LSP, and are not covered in [24].

In the limit of gluino dominance, we expect iso-contours of bounds on λ'_{111} from $0\nu\beta\beta$ to depend mostly on $M_{1/2}$. On the other hand, if the slepton-neutralino terms dominate contributions to $M_{\lambda'_{111}}$, bounds on λ'_{111} from this process should depend more sensitively on M_0 . In fact, we see in fig. 11 that the iso-contours show a non-trivial dependence on both M_0 and $M_{1/2}$. The main reason for this is that the running squark masses receive large corrections due to renormalisation effects from the gluino. This pushes both the gluino and

⁵Note the excluded parameter space for panel a) is different from the other panel in this region. In panel a), this excluded region is based on LEP bound on chargino and smuon production cross section and chargino mass.

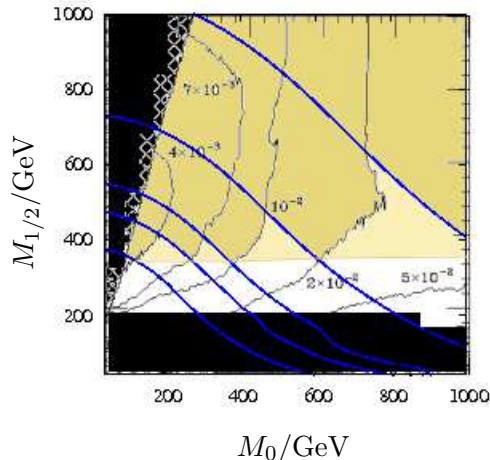


Figure 12: Parameter space in which single selectron production may be observed at the LHC, assuming $T_{1/2}^{0\nu\beta\beta}(^{76}\text{Ge}) = 1.9 \cdot 10^{25}$ yrs and $m_{\beta\beta} = 0$. The plot is obtained by overlaying fig. 11(a) on top of fig. 11(b). Regions where $0\nu\beta\beta \lambda'_{111}$ bound is larger than the discovery reach contours are coloured in dark yellow. The light yellow regions are obtained by interpolating between intersections of the two sets of contours. Due to the strong dependence of the $0\nu\beta\beta \lambda'_{111}$ bound on SUSY mass scale, the $0\nu\beta\beta$ bound relaxes rapidly as the SUSY scale goes up, leading to good single selectron discovery potential already at moderate $M_{1/2}$. In this plot, $A_0 = 0$ and $\tan\beta = 10$ is assumed.

the squark masses much higher compared with the slepton and the neutralinos, thus partially compensating the strength of the strong interaction and making contributions from the gluino and the neutralino amplitudes comparable in a significant region of parameter space. This should be compared with works in the literature [1, 2], which take limits of either the gluino or the neutralino contribution to dominate when obtaining bounds on λ'_{111} .⁶

In fig. 12, we compare directly the discovery reach of $\lambda'_{2(1)11}$ with the $0\nu\beta\beta$ bound using a current limit of $T_{1/2}^{0\nu\beta\beta} = 1.9 \cdot 10^{25}$ yrs for ^{76}Ge . This figure is obtained by laying fig. 11(a) on top of fig. 11(b). The parameter space with $0\nu\beta\beta$ bound larger than the LHC discovery reach is coloured in yellow. The dark yellow region is obtained by directly comparing the two sets of contours, while the light yellow region is obtained by interpolating between intersections of these contours. We see that if $0\nu\beta\beta$ is just beyond the current experimental reach, and is dominated by λ'_{111} , then an mSUGRA like mass spectrum with moderate $M_{1/2} \sim 350$ GeV already leads to good prospects of single selectron production observation at the LHC. Also, for higher SUSY mass scales, single selectron production is discoverable for larger ranges of λ'_{111} . We stress that this is because of the strong scaling relation of the upper λ'_{111} bound with SUSY mass scale displayed in eq. (3.10). At small $M_{1/2}$, the gluino and squark masses will be lower, substantially increasing their contributions to $0\nu\beta\beta$ via

⁶The authors' focus is not so much on the effects of mass spectrum on the λ'_{111} bound as on the NME calculation.

the gluino diagrams, thus making the bound on λ'_{111} very stringent.

If $0\nu\beta\beta$ is marginally observed at the limit of the next round of $0\nu\beta\beta$ experiments, the contribution from $m_{\beta\beta}$ may not be neglected consistently. For ^{76}Ge , a reach of $T_{1/2}^{0\nu\beta\beta} \sim 10^{27}\text{yrs}$ implies that an inverted or quasi-degenerate neutrino mass spectrum may contribute to $0\nu\beta\beta$ at an observable level.⁷ Whether it interferes with the direct contribution amplitude constructively or not will become important in setting bounds on λ'_{111} and hence the potential observability at the LHC. We show in fig. 13 the contours of upper bounds on λ'_{111} assuming an observed half life of ^{76}Ge of $1.0 \cdot 10^{27}\text{yrs}$, with constructive and destructive interference between the $m_{\beta\beta}$ contribution and the direct contributions, assuming that $|m_{\beta\beta}| = \sqrt{\Delta m_{atm}^2} \sim 0.05\text{eV}$. The colour code is the same as fig. 12. We see that for the case of constructive interference in fig. 13(c), discovery of single slepton production becomes very difficult with 10fb^{-1} of data. On the other hand, the situation improves substantially if destructive interference occurs instead. This is shown in fig. 13(d). We see that single selectron production may be observed for $M_{1/2} \gtrsim 500\text{ GeV}$. If the neutrino mass spectrum is instead normal hierarchical, the $m_{\beta\beta}$ diagram will be sub-dominant for the half life discussed above. This situation may be approximated by setting $m_{\beta\beta} = 0$ and is shown in fig. 13(b), and is the limit taken in Ref. [33], where the prospect of linking single slepton production with neutrinoless double beta decay was first introduced.

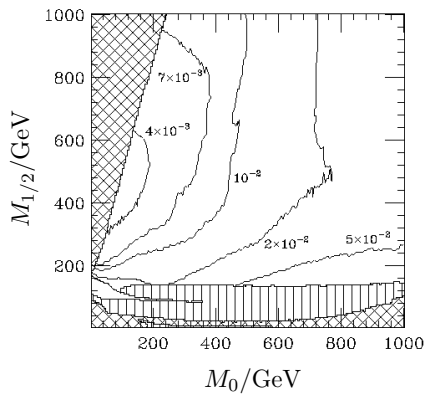
6. Discussion and summary

In this paper we have discussed the interplay between a number of observables in RPV SUSY: neutrinoless double beta decay, $B_d^0\text{-}\bar{B}_d^0$ mixing, single slepton production at the LHC, and neutrino masses. We see that while it is difficult to unambiguously infer RPV effects from separate observations, the combined knowledge of these results may allow us to deduce specific RPV contributions to the observables. It should be stressed then that even though we have chosen to concentrate on the impact of RPV physics on neutrinoless double beta decay from other (potential) observations/constraints, the discussion can easily go in the opposite direction.

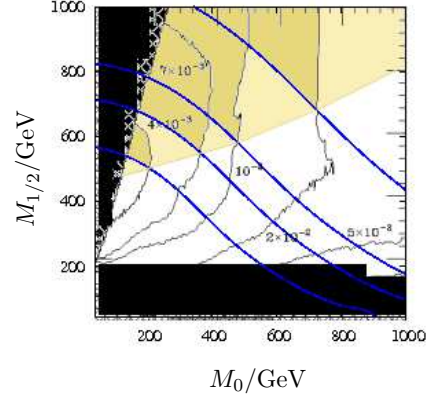
As we have seen in previous sections, bounds from $B_d^0\text{-}\bar{B}_d^0$ mixing and single slepton production could constrain the extent to which the $\lambda'_{113}\lambda'_{131}$ and $\lambda'_{111}\lambda'_{111}$ contributions may be responsible for $0\nu\beta\beta$. For the $\lambda'_{113}\lambda'_{131}$ contribution, we have pointed out a discrepancy between the effective Lagrangian used for many NME calculations and have written down the correct Lagrangian at the quark level. Comparison is made with the $0\nu\beta\beta$ bound. If the B meson mass difference receives contributions from $\lambda'_{113}\lambda'_{131}$ comparable to those coming from the SM, the current experimental bound implies that this mechanism could still lead to $T_{1/2}^{0\nu\beta\beta}$ of $\sim 10^{26}\text{yrs}$, thus being potentially observable in future 100kg $0\nu\beta\beta$ experiments.

However, the above expectation is subject to significant uncertainties from the NME. This difference is important because the sensitivity of the next round of $0\nu\beta\beta$ ^{76}Ge experiments is not expected to go far beyond the 10^{27} yrs level. In the large NME limit, the

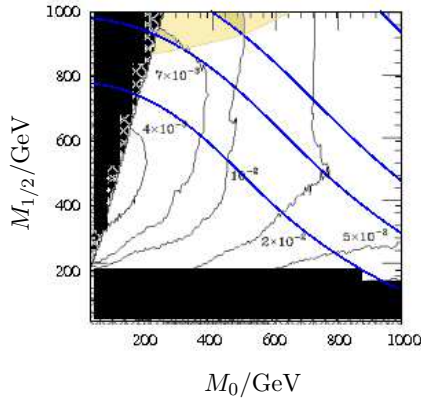
⁷It is perhaps natural to consider the case where the neutrino mass matrix arises as a RPV effect once one allows the presence of RPV couplings to mediate $0\nu\beta\beta$. We explore this issue further in appendix A.



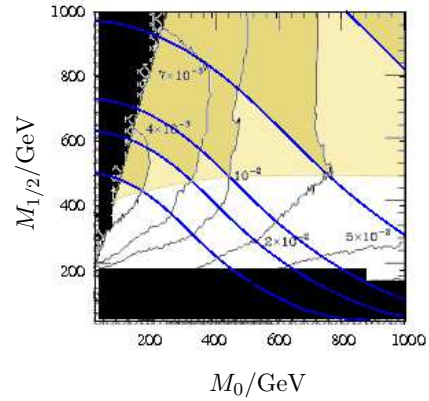
(a) Discovery reach of $\lambda'_{2(1)11}$, from [24].



(b) $T_{1/2}^{0\nu\beta\beta}({}^{76}\text{Ge}) = 1.0 \cdot 10^{27}$ yrs, $m_{\beta\beta} = 0$



(c) $|m_{\beta\beta}| = 0.05\text{eV}$, constructive interference



(d) $|m_{\beta\beta}| = 0.05\text{eV}$, destructive interference

Figure 13: As fig. 11 and fig. 12, but for a $0\nu\beta\beta$ half life $T_{1/2}^{0\nu\beta\beta}$ of $1.0 \cdot 10^{27}$ yrs for next generation experiments. Fig. 13(b) shows the regions where single selectron production may be observed with $m_{\beta\beta} = 0$, whereas figs. 13(c) and 13(d) show how this would change when $|m_{\beta\beta}| = 0.05$ eV, with constructive and destructive interference respectively. The colour code is the same as in fig. 12. In these plots, $A_0 = 0$ and $\tan\beta = 10$ are assumed.

$B_d^0-\bar{B}_d^0$ constraint will provide no comparable limit on $\lambda'_{113}\lambda'_{131}$ if the sparticles contributing to $0\nu\beta\beta$ as well as $B_d^0-\bar{B}_d^0$ mixing have similar masses. In this sense it is interesting to observe that the bounds from $0\nu\beta\beta$ and $B_d^0-\bar{B}_d^0$ are comparable in regions with 0.1–1 TeV scale SUSY breaking, with the latter one slightly more stringent in the parameter space we explored. The inclusion of pion modes is expected to increase the total NME, thus improving the sensitivity of $0\nu\beta\beta$ compared with the $B_d^0-\bar{B}_d^0$ constraints.

Given recent experimental and theoretical progress in $B_d^0-\bar{B}_d^0$ mixing, more stringent bounds on new physics from this observable is expected in the future. A recent result from [67] suggests that new physics contributions to $B_d^0-\bar{B}_d^0$ with magnitude similar to the SM contribution are still allowed. Improvements in this situation affect the upper bound

on $\lambda'_{113}\lambda'_{131}$ strongly. As the lower $0\nu\beta\beta$ limit of ^{76}Ge from $B_d^0\text{-}\bar{B}_d^0$ bound obtained in this study is in the region of $10^{26} - 10^{27}$ yrs in large regions of parameter space, not far below the $T_{1/2}^{0\nu\beta\beta}$ reach of the next round of experiments, improvements on $B_d^0\text{-}\bar{B}_d^0$ mixing calculation, as well as limiting the uncertainty in NME calculations would be very beneficial.

Turning the argument around, if $0\nu\beta\beta$ is observed at $\lesssim 10^{27}$ yrs level, the assumption of sbottom exchange as the dominant decay mechanism implies fairly low masses of the sbottom and the selectron neutrinos, which could potentially be obtained in collider experiments. We note here that even though the analysis performed in this work is restricted to an mSUGRA plane, the applicability of the result may be extended to other parameter regions, in the sense that only the sbottom and sneutrino mass matrices are relevant in comparing $0\nu\beta\beta$ and $B_d^0\text{-}\bar{B}_d^0$ mixing limits on $\lambda'_{113}\lambda'_{131}$. While it may be possible to obtain further supporting evidence from other strategies, for example by comparing life times of different nuclei [34], it would be difficult to obtain direct information on the *individual* values of λ'_{113} and λ'_{131} at the LHC, due to the difficulties in separating quark flavours for instance. Of course, $\lambda'_{113}\lambda'_{131}$ could simply be absent or highly suppressed due to some (unspecified) high scale flavour physics model.

For the λ'_{111} contribution, we have corrected certain terms in the effective Lagrangian at the quark level, that were incorrect in the literature. We point out that, contrary to previous expectations, the same sign di-lepton signal from single selectron production via gauge decay at the LHC could be observed, despite the stringent bound from $0\nu\beta\beta$. This is possible because the constraint from $0\nu\beta\beta$ on λ'_{111} relaxes rapidly as SUSY scale increases. Our comparison of the λ'_{111} bound from $0\nu\beta\beta$ with the LHC reach of λ'_{111} in the literature shows that if a direct contribution via λ'_{111} is the dominant $0\nu\beta\beta$ mechanism, there is a good chance of observing single selectron production at the LHC even with only 10fb^{-1} of data for $M_{1/2} \gtrsim 350$ GeV, if $0\nu\beta\beta$ of ^{76}Ge is just beyond current reach. By comparing the value of λ'_{111} obtained from the collider to the (non-) observation of $0\nu\beta\beta$, it may even be possible to gain information on the neutrino mass spectrum.

Acknowledgement

This work has been partially supported by STFC. We thank the members of the Cambridge SUSY working group and G. Hiller, M. Hirsch and R. Mohapatra for valuable conversations. CHK is funded by a Hutchison Whampoa Dorothy Hodgkin Postgraduate Award. HP was partially funded by the EU project ILIAS N6 WP1. BCA and CHK also thank the Technische Universität Dortmund, and HP thanks the University of Cambridge for hospitality offered while part of this work was carried out.

A. Neutralino decays with RPV couplings associated with the neutrino mass scale

In the study of single slepton production, typically the coupling responsible for the production is assumed to be the only non-zero RPV parameter in the effective SUSY Lagrangian.

However this assumption ceases to hold if neutrino masses owe their origin to RPV couplings. The presence of additional RPV couplings could significantly affect the analysis on the discovery reach of λ'_{111} . An extreme example would be when a neutralino LSP decays dominantly via λ'_{i33} , leading to either two b-jet final states plus missing energy, or a lepton, b jet plus a top, the latter of which decays through Standard Model interactions. Depending on the RPV coupling responsible for the neutrino masses, these couplings may also significantly affect other sparticle decays compared with the RPC limit. Constraints on various RPV couplings from neutrino data may be found in [11, 31, 57–60, 68–74]. In single slepton search with the same sign di-lepton signal, it is important to make sure that the resonant particle produced does not immediately decay via a RPV coupling, but decays instead via gauge interaction to the neutralino LSP. In general, the smallness of the neutrino mass scale as well as various lepton flavour/number violating constraints limit the RPV couplings to be small⁸ [31]. There exist many interactions in the RPV sector which can contribute to neutrino masses at the atmospheric scale $\sqrt{\Delta m_{atm}^2}$, but are too small to affect sparticle decays except for that of the LSP. If the LSP partial widths from these couplings are small compared with the ones from λ'_{111} , the analysis on a single slepton search in [24] should still be applicable. There are at least 8 parameters, λ'_{i33} , λ_{i33} and κ_i (where $i = 1, 2, 3$) in this category, and it is expected that they are sufficient to construct neutrino masses consistent with the neutrino oscillation data. Even if the LSP partial widths from these couplings dominate over that from λ'_{111} , as long as they give rise to the same final states, i.e. 2 jets plus 1 electron, and they do not affect the decay chain of other sparticles, the analysis should also go through without many modifications. In the parameter space (3.12) we explore, we fix λ'_{i22} to give $\Delta m_{atm}^2 \sim 0.05$ eV. The largest value it takes is $\lambda'_{i22} = 0.011$ at high M_0 and $M_{1/2}$. λ'_{i22} gives the same final state as in our analysis since flavour jets is not measured. However, λ'_{222} and λ'_{322} will reduce the number of events in the signal channel.

To estimate the extent to which other RPV couplings may affect the decay of the LSP, the ratio of partial widths of the neutralino LSP from various RPV couplings compared to that of λ'_{111} is shown in fig. 14. In fig. 14(a), we show the ratio of the sum of partial widths from λ'_{i33} , λ_{i33} and κ_i , where $i = 2, 3$, to the partial width from λ'_{111} . The former 3 sets of couplings are set such that individual coupling leads to neutrino mass scales of order $\sqrt{\Delta m_{atm}^2}$. To calculate the partial widths, the values of the RPV couplings are first obtained by a neutrino mass code [61] embedded in an RPV version of SOFTSUSY. These parameters, together with the mass spectrum are then interfaced to ISAJET 7.64 [75] via WIGISASUSY in order to calculate 3 body partial widths of the lightest neutralino. For the 2 body decay via bilinear RPV couplings, we calculate the lightest neutralino partial widths using tree level Lagrangian parameters. The code is checked against ISAJET 7.64 for the 2 body decay of the higgsino like neutralinos via the RPC bilinear parameters. As can be seen, their branching ratios only contribute a small fraction to the total partial width, and their effect on decay of sparticles higher up in the chain is expected to be negligible. For the trilinear RPV couplings, this is because the neutrino masses arising from these

⁸Many of these bounds limit specific coupling *products*, so it is possible to envisage ‘unpaired’ large RPV couplings and significantly change the results of the single slepton analysis. We neglect these scenarios here.

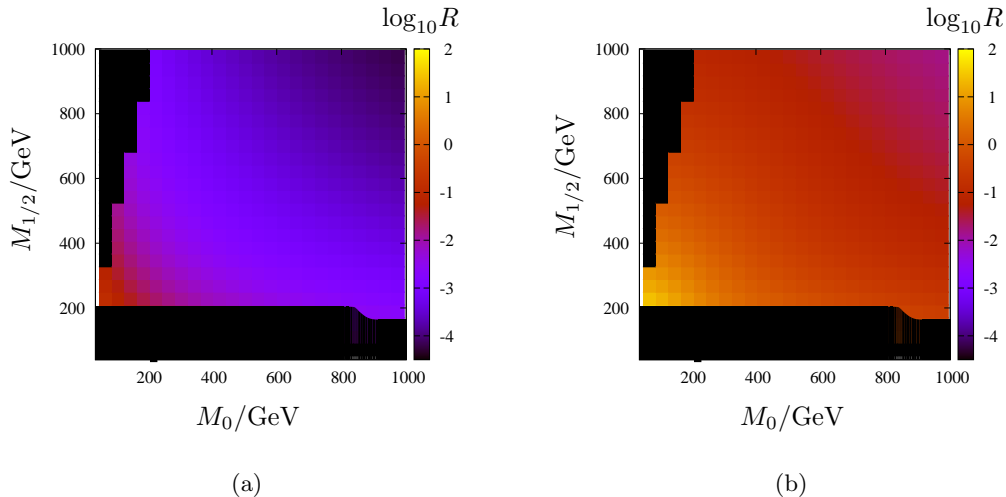


Figure 14: Colour plots showing the ratio R of the sum of LSP partial widths from a selected set of RPV couplings to the partial width from λ'_{111} . In fig. 14(a), the RPV couplings involved are λ'_{i33} , λ_{i33} and κ_i with $i = 2, 3$. In fig. 14(b), the couplings λ'_{222} and λ'_{322} are considered. The value of λ'_{111} is set to be the upper bound from current $0\nu\beta\beta$ constraint. For all other couplings, their values are set to correspond to the atmospheric neutrino mass scale. In the above plots, $A_0 = 0$ and $\tan\beta = 10$ is assumed.

couplings are proportional to the quark mass and left-right squark mass mixing in the loop. The suppression of the bilinear parameters comes from the so-called electroweak see-saw in the 7×7 neutrino-neutralino mass matrix. This suppression also appears in the 2 body decay of the neutralino, and the partial width is further suppressed by the mass of the W/Z bosons. For the case of λ'_{222} and λ'_{322} , the ratio of partial widths to that of λ'_{111} is displayed in fig. 14(b). Here the two partial widths are comparable in magnitude.

References

- [1] M. Hirsch, H. V. Klapdor-Kleingrothaus and S. G. Kovalenko, Phys. Rev. D **53**, 1329 (1996) [arXiv:hep-ph/9502385].
- [2] A. Faessler, S. Kovalenko and F. Simkovic, Phys. Rev. D **58** (1998) 115004 [arXiv:hep-ph/9803253].
- [3] M. Hirsch, H. V. Klapdor-Kleingrothaus and S. G. Kovalenko, Phys. Lett. B **372**, 181 (1996) [Erratum-ibid. B **381**, 488 (1996)] [arXiv:hep-ph/9512237].
- [4] H. Päs, M. Hirsch and H. V. Klapdor-Kleingrothaus, Phys. Lett. B **459**, 450 (1999) [arXiv:hep-ph/9810382];
- [5] A. Faessler, T. Gutsche, S. Kovalenko and F. Simkovic, arXiv:0710.3199 [hep-ph].
- [6] J. L. Goity and M. Sher, Phys. Lett. B **346** (1995) 69 [Erratum-ibid. B **385** (1996) 500] [arXiv:hep-ph/9412208].
- [7] G. R. Farrar and P. Fayet, Phys. Lett. B **76** (1978) 575.

- [8] N. Sakai and T. Yanagida, Nucl. Phys. B **197** (1982) 533.
- [9] S. Weinberg, Phys. Rev. D **26** (1982) 287.
- [10] L. E. Ibanez and G. G. Ross, Phys. Lett. B **260** (1991) 291.
- [11] H. K. Dreiner, J. Soo Kim and M. Thormeier, arXiv:0711.4315 [hep-ph].
- [12] A. Dedes, S. Rimmer and J. Rosiek, JHEP **0608**, 005 (2006) [arXiv:hep-ph/0603225].
- [13] A. S. Joshipura and S. K. Vempati, Phys. Rev. D **60** (1999) 111303 [arXiv:hep-ph/9903435].
- [14] A. S. Joshipura and M. Nowakowski, Phys. Rev. D **51** (1995) 2421 [arXiv:hep-ph/9408224].
- [15] M. Nowakowski and A. Pilaftsis, Nucl. Phys. B **461** (1996) 19 [arXiv:hep-ph/9508271].
- [16] Y. Grossman and S. Rakshit, Phys. Rev. D **69** (2004) 093002 [arXiv:hep-ph/0311310].
- [17] Y. Grossman and H. E. Haber, Phys. Rev. Lett. **78** (1997) 3438 [arXiv:hep-ph/9702421].
- [18] Y. Grossman and H. E. Haber, Phys. Rev. D **59** (1999) 093008 [arXiv:hep-ph/9810536].
- [19] S. Davidson and M. Losada, JHEP **0005** (2000) 021 [arXiv:hep-ph/0005080].
- [20] S. Davidson and M. Losada, Phys. Rev. D **65** (2002) 075025 [arXiv:hep-ph/0010325].
- [21] D. Choudhury and P. Roy, Phys. Lett. B **378** (1996) 153 [arXiv:hep-ph/9603363].
- [22] M. Hirsch, J. C. Romao and J. W. F. Valle, Phys. Lett. B **486**, 255 (2000) [arXiv:hep-ph/0002264].
- [23] R. Barbieri, A. Strumia and Z. Berezhiani, Phys. Lett. B **407** (1997) 250 [arXiv:hep-ph/9704275].
- [24] H. K. Dreiner, P. Richardson and M. H. Seymour, Phys. Rev. D **63** (2001) 055008 [arXiv:hep-ph/0007228].
- [25] J. L. Hewett and T. G. Rizzo, arXiv:hep-ph/9809525.
- [26] J. Kalinowski, R. Ruckl, H. Spiesberger and P. M. Zerwas, Phys. Lett. B **414** (1997) 297 [arXiv:hep-ph/9708272].
- [27] B. Allanach *et al.* [R parity Working Group Collaboration], arXiv:hep-ph/9906224.
- [28] H. K. Dreiner, P. Richardson and M. H. Seymour, JHEP **0004** (2000) 008 [arXiv:hep-ph/9912407].
- [29] S. Dimopoulos, R. Esmailzadeh, L. J. Hall and G. D. Starkman, Phys. Rev. D **41** (1990) 2099.
- [30] H. K. Dreiner, S. Grab and M. K. Trenkel, arXiv:0808.3079 [hep-ph].
- [31] B. C. Allanach, A. Dedes and H. K. Dreiner, Phys. Rev. D **60** (1999) 075014. [arXiv:hep-ph/9906209].
- [32] R. N. Mohapatra, Phys. Rev. D **34** (1986) 3457.
- [33] B. C. Allanach, C. H. Kom and H. Päs, arXiv:0902.4697 [hep-ph].
- [34] F. Deppisch and H. Päs, Phys. Rev. Lett. **98** (2007) 232501 [arXiv:hep-ph/0612165].
- [35] V. M. Gehman and S. R. Elliott, J. Phys. G **34**, 667 (2007) [Erratum-ibid. **G35**, 029701 (2008)] [arXiv:hep-ph/0701099].

- [36] A. Wodecki, W. A. Kaminski and F. Simkovic, Phys. Rev. D **60** (1999) 115007 [arXiv:hep-ph/9902453].
- [37] M. Doi, T. Kotani and E. Takasugi, Prog. Theor. Phys. Suppl. **83** (1985) 1.
- [38] P. Vogel, arXiv:0807.2457 [hep-ph].
- [39] P. Minkowski, Phys. Lett. B **67** (1977) 421.
- [40] R. N. Mohapatra and G. Senjanovic, Phys. Rev. D **23** (1981) 165.
- [41] G. Lazarides, Q. Shafi and C. Wetterich, Nucl. Phys. B **181** (1981) 287.
- [42] M. Misiak, S. Pokorski and J. Rosiek, Adv. Ser. Direct. High Energy Phys. **15** (1998) 795 [arXiv:hep-ph/9703442].
- [43] B. Pontecorvo, Sov. Phys. JETP **26** (1968) 984 [Zh. Eksp. Teor. Fiz. **53** (1967) 1717].
- [44] Z. Maki, M. Nakagawa and S. Sakata, Prog. Theor. Phys. **28** (1962) 870.
- [45] K. S. Babu and R. N. Mohapatra, Phys. Rev. Lett. **75** (1995) 2276 [arXiv:hep-ph/9506354].
- [46] B. C. Allanach, Comput. Phys. Commun. **143** (2002) 305 [arXiv:hep-ph/0104145].
- [47] A. Faessler and F. Simkovic, J. Phys. G **24** (1998) 2139 [arXiv:hep-ph/9901215].
- [48] L. Baudis *et al.*, Phys. Rev. Lett. **83** (1999) 41 [arXiv:hep-ex/9902014].
- [49] H. V. Klapdor-Kleingrothaus *et al.*, Eur. Phys. J. A **12**, 147 (2001) [arXiv:hep-ph/0103062].
- [50] G. Pantis, F. Simkovic, J. D. Vergados and A. Faessler, Phys. Rev. C **53** (1996) 695 [arXiv:nucl-th/9612036].
- [51] F. Simkovic, G. Pantis, J. D. Vergados and A. Faessler, Phys. Rev. C **60** (1999) 055502 [arXiv:hep-ph/9905509].
- [52] S. R. Elliott and J. Engel, J. Phys. G **30** (2004) R183 [arXiv:hep-ph/0405078].
- [53] V. A. Rodin, A. Faessler, F. Simkovic and P. Vogel, Nucl. Phys. A **766**, 107 (2006) [Erratum-ibid. A **793**, 213 (2007)] [arXiv:0706.4304 [nucl-th]].
- [54] S. Schael, and others, Eur. Phys. J. C **47** (2006) 547-587 [arXiv:hep-ex/0602042].
- [55] H. Baer and X. Tata, “Weak scale supersymmetry: From superfields to scattering events,” *Cambridge, UK: Univ. Pr. (2006) 537 p*
- [56] S. Rakshit, G. Bhattacharyya and A. Raychaudhuri, Phys. Rev. D **59** (1999) 091701 [arXiv:hep-ph/9811500].
- [57] A. Abada and M. Losada, Phys. Lett. B **492** (2000) 310 [arXiv:hep-ph/0007041].
- [58] A. Abada, G. Bhattacharyya and M. Losada, Phys. Rev. D **66** (2002) 071701 [arXiv:hep-ph/0208009].
- [59] M. Hirsch, M. A. Diaz, W. Porod, J. C. Romao and J. W. F. Valle, Phys. Rev. D **62** (2000) 113008 [Erratum-ibid. D **65** (2002) 119901] [arXiv:hep-ph/0004115].
- [60] M. A. Diaz, M. Hirsch, W. Porod, J. C. Romao and J. W. F. Valle, Phys. Rev. D **68** (2003) 013009 [Erratum-ibid. D **71** (2005) 059904] [arXiv:hep-ph/0302021].
- [61] B. C. Allanach and C. H. Kom, JHEP **0804** (2008) 081 arXiv:0712.0852 [hep-ph].
- [62] M. C. Gonzalez-Garcia and M. Maltoni, arXiv:0704.1800 [hep-ph].

- [63] W. M. Yao et al., *Particle Data Group*, Journal of Physics G **33**, 1 (2006) <http://pdg.lbl.gov/>.
- [64] H. V. Klapdor-Kleingrothaus, H. Päs and A. Y. Smirnov, Phys. Rev. D **63** (2001) 073005 [arXiv:hep-ph/0003219].
- [65] M. Fukugita, K. Ichikawa, M. Kawasaki and O. Lahav, Phys. Rev. D **74** (2006) 027302 [arXiv:astro-ph/0605362].
- [66] J. Charles *et al.* [CKMfitter Group], Eur. Phys. J. C **41** (2005) 1 [arXiv:hep-ph/0406184].
- [67] O. Deschamps, arXiv:0810.3139 [hep-ph].
- [68] J. C. Romao, M. A. Diaz, M. Hirsch, W. Porod and J. W. F. Valle, Phys. Rev. D **61** (2000) 071703 [arXiv:hep-ph/9907499].
- [69] A. Abada, S. Davidson and M. Losada, Phys. Rev. D **65** (2002) 075010 [arXiv:hep-ph/0111332].
- [70] D. E. Kaplan and A. E. Nelson, JHEP **0001** (2000) 033 [arXiv:hep-ph/9901254].
- [71] B. C. Allanach, A. Dedes and H. K. Dreiner, Phys. Rev. D **69** (2004) 115002 [Erratum-ibid. D **72** (2005) 079902] [arXiv:hep-ph/0309196].
- [72] A. Datta, J. P. Saha, A. Kundu and A. Samanta, Phys. Rev. D **72** (2005) 055007 [arXiv:hep-ph/0507311].
- [73] R. Hempfling, Nucl. Phys. B **478** (1996) 3 [arXiv:hep-ph/9511288].
- [74] E. J. Chun, S. K. Kang, C. W. Kim and U. W. Lee, Nucl. Phys. B **544** (1999) 89 [arXiv:hep-ph/9807327].
- [75] F. E. Paige, S. D. Protopopescu, H. Baer and X. Tata, arXiv:hep-ph/0312045.